A New Hyper-Laplacian Prior-Based Deconvolution Method for Single Image Deblurring

[1]Chia-Feng Chang and [2, *]Jiunn-Lin Wu

Abstract

Motion blur is an ill-posed problem which has been addressed for a long time in digital photographing. It usually happens under the circumstance without enough surrounding light. Several methods have been proposed for this problem. However, the ringing is inevitable artifacts arising in the deconvolution stage. To suppress undesirable artifacts, regularization-based methods have been proposed, and they use the natural image priors to overcome the ill-posedness of deconvolution problems. These studies suggest that priors based on natural image statistics can regularize deblurring problems to yield better results.

In this paper, we propose a new single image deblurring algorithm based on the hyper-Laplacian priors. We apply hyper-Laplacian priors to obtain a precise blur kernel in the point spread function (PSF) estimation phase. Our proposed method successfully reduces ringing artifacts while preserving the edge of images. Experimental results simulated and real images show that our method performs better than other methods.

Keywords: Image Deconvolution, Hyper-Laplacian Priors, Shock Filter, Blind Deconvolution, Maximum a Posteriori.

1. Introduction

In past decade, image deblurring has become an important issue owing to the popularity of hand-held camera and smart phone. Under the dark environment, the movement of camera may cause motion blur happened in the image during photo capturing. The movement of cameras can be viewed as a blur kernel called point spread function (PSF). If PSF is shift-invariant, the deblurring problem can be reduced to an image deconvolution problem. According to known PSF, the image deconvolution can be separated into two types, non-blind image deconvolution and blind image deconvolution. In non-blind deconvolution, the PSF is known; therefore blurred image with motion blur can be well recovered. Wiener filter [1] and Richardson-Lucy deconvolution [2] are well-known non-blind deconvolution algorithms which are good at image deblurring while PSF is not complicated. But in real cases, the PSF is unknown and more complex. If PSF is not estimated accurately enough, the deblurring process will fail. To estimate an accurate PSF is an important issue for image deblurring problems. Blind deconvolution estimates PSF and restores the blurred images simultaneously. However, this problem can be more ill-posed because of unknown PSF and latent images. Image pair approaches [3-6] have been proposed for image deblurring. Leveraging additional images makes blind deblurring problem more tractable. Rav-Acha et al. used two motion blur images [3]. Yuan et al. used noise/motion pair to capture at low light condition to recover blurred images [4]. Zhuo et al. leverages flash/motion pair which provides clear structure information for image deblurring problems [5]. However, image pair approach needs additional images captured by an extra hardware, but single image approach does not need. In 2006, Fergus proposed a maximum a posterior (MAP) based on a blind image deconvolution method [7] to well recover blurred image. Fergus only considered the edge region of blurred image. Therefore the ringing artifacts often appear at smooth regions in the deblurred image. In 2008, Shan successfully reduced the ringing artifacts using local prior which indicates smooth regions and edge regions [8]. However, numbers of priors make the progress of image deblurring too complicated to efficiently deblur a blurred image. In 2009, Cho proposed that shock filter and fast Fourier transform is used to accelerate the deblurring process [9]. Therefore, the time complexity of Cho's method can be significantly reduced. However, it doesn't consider the statistical information of real-world images; this may lead to undesired result. In fact, studies of real-world images show that the marginal distribution is heavy-tailed [10]. And [11] suggests that estimating PSF alone can recover more accurate PSF.

In this paper, we proposed a hyper-Laplacian based image deblurring method. First, image filters are performed to predict important information for the image deblurring process and remove enhanced noises. A shock filter is a good tool to restore a larger step. We apply a shock filter to restore a step edge in the blurred image. However, the noise is also

*Corresponding Author: Jiunn-Lin Wu
(E-mail: jlwu@cs.nchu.edu.tw)
[1]Department of Computer Science and Engineering, National Chung Hsing University, 402 Taichung, Taiwan
[2]Department of Computer Science and Engineering, National Chung Hsing University, 402 Taichung, Taiwan

enhanced. Bilateral filter is then applied to remove enhanced noises. After obtaining an initial restored image, MAP approach is used to perform the optimization process. For reducing ringing artifacts and better image visual perspective, we applied hyper-Laplacian priors into the optimization function in PSF estimation phase. Then we take the conjugate gradient (CG) method to solve the equation derived from the optimization function.

This paper is organized as follows. Section 2 reviews the related work including PSF estimation and latent image recovery methods. The proposed method is described in Section 3. In Section 4, both synthesized and real images are used to measure the performance. Finally, the conclusions are given in Section 5.

2. Related works

Removing ringing artifacts is an important issue in image deblurring. Many researches have been proposed to address this problem, including image pair deblurring algorithms and single image deblurring algorithms. Image pair deblurring algorithms have better performance in deblurred results, but image pair deblurring methods need additional image to help recovering clear images. Additional images such as flash images and blurry images need an extra hardware to be acquired. Therefore, in this paper we focus on single image deblurring algorithms.

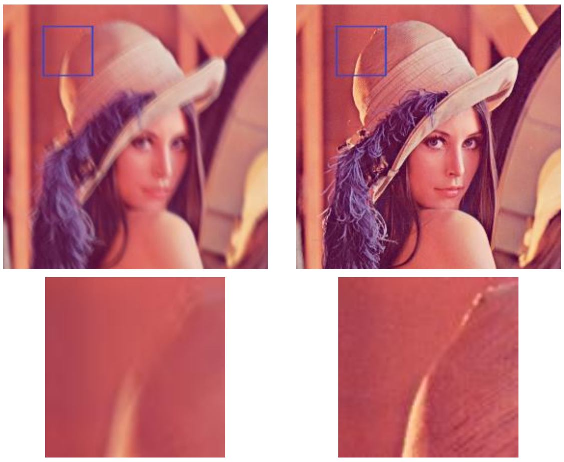

(a) (b)

Figure 1: Example of local priors. (a) Blurred image. (b) Original unblurred image. The first row is full size images and the second row is the close-up views corresponding to the blue rectangle in the first row images. From this example, we can notice that smooth regions of the blue rectangle in blurred image are also smooth in original image. We use this information as local priors for image deblurring.

In 2008, Shan et al. computed a deblurred image using a unified probabilistic model of both blur PSF estimation and latent image recovery. The method is effective to handle a more general motion blur given from a single image. During a latent image deconvolution stage, Shan designed two components for an image prior term to reduce the ringing artifacts, global priors and local priors. The global priors are emphasized to encourage the reconstruction of edges according to the gradient heavy-tailed distribution. Another one is the local priors. This novel prior term uses the blurry property to constrain the gradient to be similar to the unblurred latent image gradient. Figure 1 shows that locally smooth regions of image will be still smooth after blurring, but the smoothing differs across the image, and the edge will be affected. Local priors clearly help suppress ringing which might induce incorrect image structures and confuse the PSF estimation. However, the complexity probability model makes the optimization process more difficult. In 2009, Cho et al. applied the shock filter to accelerate the progress of optimization. The strong edges are predicted from the estimated latent image using a shock filter. And then the predicted latent image is used to estimate PSF. This approach avoids using complicated and inefficient priors to estimate latent image. Cho further reduces process time by using image pyramid so that the time complexity can be significantly reduced. However, during the optimization process, Cho's method doesn't consider the information of real-world images where the distribution of image gradient is heavy-tailed; this may cause the ringing artifact happened in the deblurred image.

Priors based on natural image statistics can regularize deblurring problems to yield better results. The heavy-tailed distributions of gradients in natural scenes have proven advanced priors for a range of restoration problems. These distributions are well modeled by a hyper-Laplacian, as shown in Figure 2.

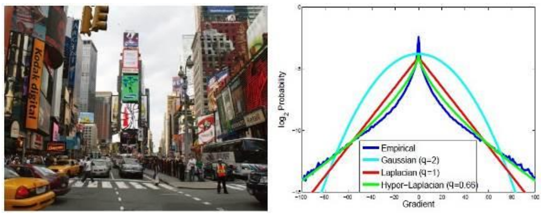

(a) (b)

Figure 2: The heavy-tailed characteristic of gradients in natural scenes. The x-axis is gradient magnitudes and y-axis has a logarithmic scale. (a) A real-world scene. (b) The empirical distribution of gradient magnitudes within the scene is shown in blue. And a hyper-Laplacian with exponent $2/3$ is a better model of gradients than a Laplacian or a Gaussian. Note that the hyper-Laplacian of green line fits the empirical distribution closely, particularly in the tails [10].

3. Proposed Method

In this section, we first analyze the motion blur and ringing artifacts, and the proposed image deblurring algorithm is then introduced.

In the proposed method, the procedure is mainly divided into two steps, PSF estimation phase and fast adaptive deconvolution. The proposed method follows the procedure that PSF estimation phase estimates accurate PSF, and then fast adaptive deconvolution is performed to recover clear images. Traditional image deblurring algorithms take long time to estimate PSF because of large matrices and vectors. To speed up the PSF estimation phase, we use the shock filter to predict the strong step edges of latent images. Strong step edges provide accurate information for optimization process. This can avoid local minimum solution. However, noises in blurred images are also enhanced by shock filters. Enhanced noises may lead to the failure of deblurred results. To avoid the influence of enhanced noises, we use the bilateral filter to remove noises. Next we use this predicted latent image to estimate PSF. For reducing ringing artifacts, we apply hyper-Laplacian priors to optimization process in the deconvolution step. Hyper-Laplacian priors provides heavy-tailed distribution gradient which is close to nature images. This property leads to the result of less ringing artifacts happened in deblurred images. The flow chart of proposed method is shown in Figure 3.

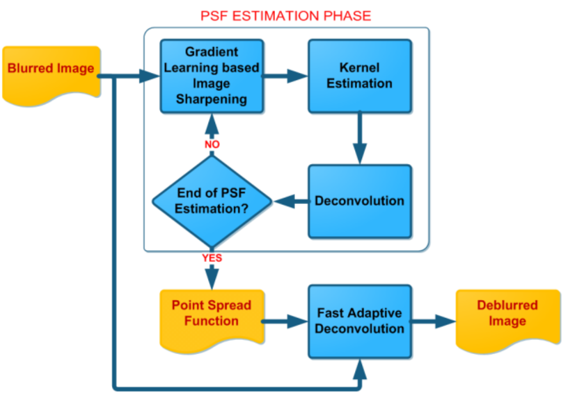

Figure 3: The Flow chart of proposed method.

3.1 PSF Estimation

Shock filter is an efficient tool for sharping blurred images. The formulation of a shock filter is defined as following

$$I_{t+1} = I_t - sign(\Delta I_t)\|\nabla I_t\|dt \qquad (1)$$

where I_t is the image at current iteration, I_{t+1} is the image at next iteration, ΔI_t is the map derived from Laplacian operator at iteration t, ∇I_t is the gradient of I at current iteration, and dt is time step. Shock filter converts blurred images into sharper images, but not the true unblurred images. In fact, shock filter just enhances blurred images, not restores blurred images, but it provides important information for well recovering the blurred image. MAP is an efficient optimization approach for solving such an optimization problem.

A blurred image can be modeled as

$$B = L * K + N \qquad (2)$$

where B is blurred image, $*$ is convolution operator, L is latent unblurred image, and K is PSF and N is noise in image.

Then the equation can be represented as follow by Bayes' theorem

$$p(L,K \mid B) \propto p(B \mid L,K)p(L)p(K) \qquad (3)$$

where $p(B \mid L,K)$ represents the likelihood, and $p(L)$, $p(K)$ denote the priors on the latent image and PSF. In PSF estimation step, the Bayes' theorem can be transformed into following equations.

$$K' = \arg\min_K \{\|K * L - B\| + p_K(K)\} \qquad (4)$$

$$L' = \arg\min_L \{\|K * L - B\| + p_L(L)\} \qquad (5)$$

Above cost functions can be rewritten as

$$f_K(K) = \sum_{\partial_*} \omega^* \|K * \partial_* L - \partial_* B\|^2 + \beta\|K\|^2 \qquad (6)$$

$$f_L(L) = \sum_{\partial_*} \omega^* \|K * \partial_* L - \partial_* B\|^2 + \alpha\|\nabla L\|^2 \qquad (7)$$

where α and β are two predefined parameters. $\partial_* \in \{\partial_0, \partial_x, \partial_y, \partial_{xx}, \partial_{xy}, \partial_{yy}\}$ is a set consisting of all the partial derivatives, and $\omega_* \in \{\omega_0, \omega_1, \omega_2\}$ are weighting values for different order of partial derivatives. We iteratively solve above equations to get accurate PSF. Many studies suggest that prior based on natural image statistics can regularize deblurring problems to yield better results. As result, we utilize the hyper-Laplacian priors to regularize the solution. Hyper-Laplacian priors can be modeled as

$$p_L(L) \propto e^{-\alpha \sum_{k=1}^{2} |f_k * L|^q} \text{ with } 0.5 \le q \le 0.8. \qquad (8)$$

where q is a positive exponent value which was suggested by Krishnan et al. [10]. In this work, we unify to use $2/3$ for q value. And f_k denotes the simple horizontal and vertical first-order derivative filters. It can also be useful to include second order derivative filters, or the more sophisticated filters. With the Gaussian noise likelihood and the hyper-Laplacian image priors, Eq. (7) can be represented by the following minimization problem

$$f_L(L)=\sum_{\partial_*}\omega_*\left\|K*\partial_*L-\partial_*B\right\|^2+\eta\sum_{k=1}^{2}\left|(f_k*L)_i\right|^q \qquad (9)$$

where η is a weighted coefficient which can be adjusted, and is a set consisting of all the partial derivatives of B. Then a conjugate gradient method is used to solve the minimization problem. To further decrease the computation time, multi-resolution schema is applied. By the from-coarse-to-fine schema, it can speed up the deblurring procedure and avoid local minimum answer. The estimated PSFs at different scales are shown in Figure 4.

The effect of hyper-Laplacian priors are shown in Figure 5. In this example, the hyper-Laplacian priors clearly help to suppress ringing caused by errors in PSF estimation. In Figure 5(d), the difference map shows that hyper-Laplacian priors are effective for reducing ringing artifacts.

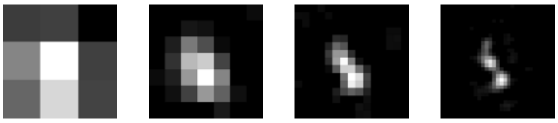

Figure 4: Estimated kernels at different image scales. When the scale becomes finer, the structure of kernel is more accurate.

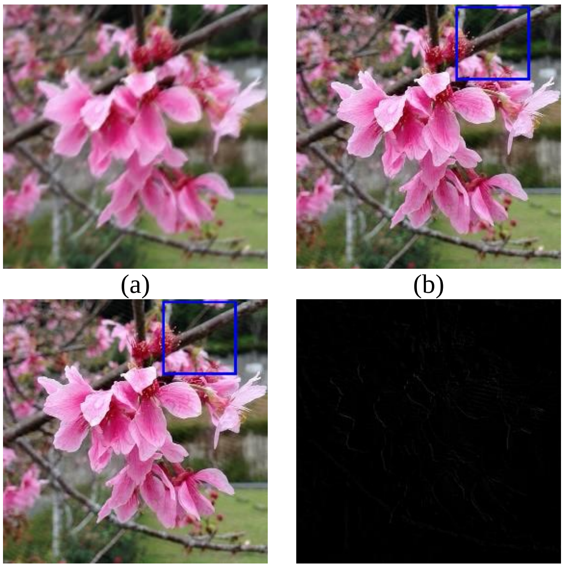

(a) (b)

(c) (d)

(e)

Figure 5: Effects of hyper-Laplacian priors. (a) Blurred image. (b) Cho's method. (c) Proposed method. (d) Color difference between Cho's method and proposed method. (e) The close-up views correspond to blue rectangle in (a) and (b). From left to right are Cho's method and proposed method. In (d), we can observe that ringing artifact has been reduced.

3.2 Final Deconvolution

When an accurate PSF is obtained, a fast adaptive deconvolution method is used for final deconvolution. Eq. (10) is the cost function of a fast deconvolution method which is proposed by Krishnan. We briefly describe the L sub-problem and its straightforward solution. Given a fixed value of ω from the previous iteration, we aim to obtain the optimal L by the following optimization problem

$$\arg\min_L\left\{\left\|K*L-B\right\|^2+\frac{\beta}{2}\left(\left(f_1*L-\omega_1\right)^2+\left(f_2*L-\omega_2\right)^2\right)\right\} \qquad (10)$$

The ω satisfying the above equation is the analytical solution of the following quartic polynomial

$$\omega^4-3v\omega^3+3v^2\omega^2-v^3\omega+\frac{\lambda_p{}^3}{27\beta^3}=0 \qquad (11)$$

To find and select the correct roots of the above quartic polynomial, we adopt Krishnan's approach, as detailed in [12].

4. Experimental Results

Our proposed algorithm is applied hyper-Laplacian priors to PSF estimation phase for reducing ringing artifacts. To verify the effectiveness of the proposed method, we use several well-known images including synthesis images and natural images as input images to verify the proposed method. These experiments are separated into two parts, synthesis images and natural images. For each part, we will perform experiment and discuss in detail. All experiments are implemented with Visual C++.Net language. The testing environment is the PC running Window 7 64bit version with AMD Phenom II X4 945 3.4 GHz. 8GB Ram.

4.1 Synthesis Images

In the synthesis image part, we will generate blurred test images and use them for experiment. Synthesis images are generated by known PSF and unblurred images. We use synthesis images for comparing the accuracy of PSF because known PSF. "*Lena*" and "*Airplane*" are used as inputs for this experiment. The size of first image "*Lena*" and its PSF are 480×480 and 33×29, as shown in Figure 6. Ringing artifacts appear around the strong edges in Cho's method, but our result shows less ringing artifacts. The size of second image "*Airplane*" and its PSF is 512×512 and 31×31, respectively, as shown in Figure 7. Comparing structure on the airplane between Cho's method and proposed method, the structure on the airplane are slightly curved while our result is not because the ringing influences the structure in Cho's result, and also the destruction at the mountains is reduced.

In addition, for testing the visual objective quality, the peak signal to noise ratio (PSNR) measurement is also used to evaluate quantitatively the quality of above restored result. Given signal I, the PSNR value of its estimate is defined as:

$$PSNR(dB)=10\cdot\log\frac{255^2}{\frac{1}{mn}\sum_{i=0}^{m-1}\sum_{j=0}^{n-1}\left(I_{ij}-\hat{I}_{uj}\right)^2} \quad (12)$$

where $m\times n$ is the size of the input image, I_{ij} is the intensity value of true clear image at the pixel location (i, j), and $\hat{I}_{ij}$ corresponds to the intensity value of the restored image at the same location. The average PSNR values of above results are listed in Table 1: Comparison of PSNRs. (Unit: dB)

(a)

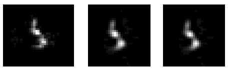

(b)

Figure 6: Deblurred result of "Lena". (a) From left to right, images are input blurred image, result of Cho's method and result of proposed method. (b) Corresponding PSF of (a). From left to right, ground truth, PSF of Cho's method and PSF of proposed method. We can observe that ringing artifact on the face of Lena is removed.

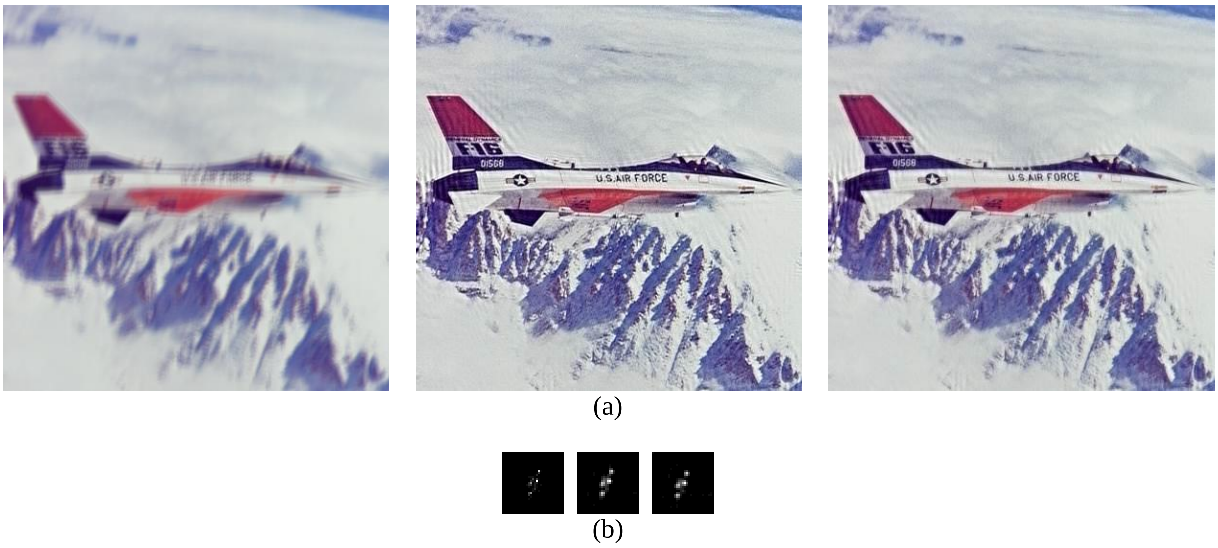

Figure 7: Deblurred result of "Airplane". (a) From left to right, images are input blurred image, result of Cho's method and result of proposed method. (b) Corresponding PSF of (a). From left to right, ground truth, PSF of Cho's method and PSF of proposed method. Compare the alphabets, the structure of alphabets in Cho's result is slightly curved and our result has better visual perspective.

In this experiment, we only use the synthesized images for test because the ground-truth exists. From Table 1, the proposed method has higher PSNRs than Cho's method, resulting that our approach has better performance than Cho's method.

Table 1: Comparison of PSNRs. (Unit: *dB*)

Image	Cho	Ours
Lena	21.6425	**22.7238**
Airplane	20.7550	**20.9608**

4.2 Real Images

In the real images part, "*Cameraman*", "*Picasso*" and "*Statue*" are used for experiments. The size of image "*Cameraman*" shown in Figure 8 is 512×512. Note that there are severe ringing artifacts around the camera in both results. However, in our deblurred result, ringing artifacts have less effect at the bottom of the camera. Then for the second image "*Statue*", its size is 688×800. From Figure 9, we notice that around the hand of left side, the ringing artifacts are reduced. The size of third image "*Picasso*" shown in Figure 10 is 800×532. Comparing the deblurred result, the ringing artifacts appear at around the old man and picture on the wall. And the same positions in our result do not suffer from undesired artifacts. Our result has more pleased image visual than Cho's method.

We also compare the proposed method with commercial software "Piccure+" [13]. "Piccure+" is a famous software program capable of correcting optical aberrations and camera shakes that cause a lack of sharpness in photos. From Figures 11 (e)(f), we can observe that our deblurred results have sharper perspective and less undesired shadow artifacts than the deblurred result of "Piccure+".

(a)

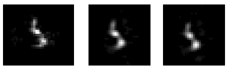

(b)

Figure 1: Deblurred result of "Lena". (a) From left to right, images are input blurred image, result of Cho's method and result of proposed method. (b) Corresponding PSF of (a). From left to right, ground truth, PSF of Cho's method and PSF of proposed method. We can observe that ringing artifact on the face of Lena is removed.

(a)

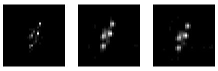

(b)

Figure 2: Deblurred result of "Airplane". (a) From left to right, images are input blurred image, result of Cho's method and result of proposed method. (b) Corresponding PSF of (a). From left to right, ground truth, PSF of Cho's method and PSF of proposed method. Compare the alphabets, the structure of alphabets in Cho's result is slightly curved and our result has better visual perspective.

(a) (b) (c)

Figure 3: Deblurred result of natural image "Camerman". (a) Blurred image and its PSF. (b) Cho's method and estimated PSF. (c) Proposed method and our estimated PSF. Ringing artifacts is slight reduced than Cho's method.

(a) (b) (c)

Figure 4: Deblurred result of "Statue". (a) Blurred image. (b) Cho's method. (c) Proposed method. We can observe that ringing artifacts on the face and around the statue are removed.

(a) (b) (c)

Figure 5: Deblurred result of natural image "Picasso". These images from left to right are (a) Blurred image. (b) Cho's method. (c) Proposed method. In our deblurred result the ringing artifact around the old man in the image is reduced.

(a)

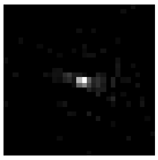

(b)

(c)

(d)

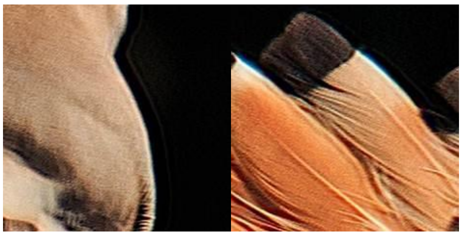

(e)

(f)

Figure 6: Deblurred result of natural image “Hoopoe”, we compared the proposed method with commercial software “Piccure+”. (a) Blurred image. (b) PSF which is estimated by proposed method. (c) Deblurred result of commercial software “Piccure+”. (d) Deblurred result of proposed method. (e) Local magnification of (c). (f) Local magnification of (d).

5. Conclusions

In this paper, we proposed a hyper-Laplacian based image deblurring method. First, the shock filter and bilateral filter are used sequentially to recover important predicted information and remove noises. For reducing ringing artifacts to get sharper images, hyper-Laplacian priors are then applied to reduce ringing artifacts in the optimization process. Finally, in order to accelerate the proposed image deburring algorithm, the multi-resolution schemas are adopted. In the experiments, both simulated and real images are used to demonstrate the performance of the proposed hyper-Laplacian-priors based method, and it shows show that our proposed method performs better than Cho’s method, and the ringing artifacts are effectively suppressed. However, we find that there still exists some ringing artifacts in deblurred images caused by the complex texture and narrow edges. How to solve this problem is our future works.

Acknowledgment

This study is supported by Ministry of science and technology, Taiwan under grants MOST 103-2221-E-005-073 and MOST 102-2221-E-005-083.

References

[1]. R. C. Gonzalez and R. E. Woods, Digital Image Processing 2nd ed., Prentice Hall, 2002.

[2]. W. H. Richardson, “Bayesian-based iterative method of image restoration,” Journal of the Optical Society of America, Vol.62, No.1, pp. 55–59, 1972.

[3]. A. Rav-Acha and S. Peleg, "Two motion-blurred images are better than one", Pattern Recognition Letters, pp.311-317, 2005.

[4]. L. Yuan, J. Sun, L. Quan, and H. Shum, "Image deblurring with blurred/noisy image pairs", ACM Trans. Graph., Vol.26, No.3, 2007.

[5]. S. Zhuo, D. Guo, and T. Sim, "Robust flash deblurring", Proc. CVPR, pp.2440-2447, 2010.

[6]. H. Zhang, D. Wipf, and Y. Zhang, "Multi-Observation Blind Deconvolution with an Adaptive Sparse Prior", IEEE Trans. PAMI, Vol. 36, No. 8, pp. 1628-1643, 2014.

[7]. R. Fergus, B. Singh, A. Hertzmann, S.T. Roweis, and W.T. Freeman, "Removing camera shake from a single photograph", ACM Trans. Graph., Vol.25, No.3, pp.787-794, 2006.

[8]. Q. Shan, J. Jia, and A. Agarwala, "High-quality motion deblurring from a single image", ACM Trans. Graph. , Vol.27, No.3, 2008.

[9]. S. Cho and S. Lee, "Fast motion deblurring", ACM Trans. Graph., Vol.28, No.5, 2009.

[10]. D. Krishnan and R. Fergus, "Fast image deconvolution using hyper-Laplacian priors", Proc. NIPS, pp.1033-1041, 2009.

[11]. A. Levin, Y. Weiss, F. Durand, and W.T. Freeman, “Understanding blind deconvolution algorithms”, IEEE Trans. Pattern Anal. Mach. Intell., Vol.33, No.12, pp.2354-2367, 2011.

[12]. J.H. Lee, and Y.S. Ho, “High-quality non-blind image deconvolution with adaptive regularization”, Journal of Visual Communication and Image Representation, Vol.22, No.7, pp.653–663, 2011.

[13]. Commercial image deblurring software “Piccure+” http://piccureplus.com/